standable that a phase cannot be leached out of pyrex glass, since an enormous pressure would be needed to force the leaching solution into such small channels. Figure 1, c and d, are photographs of pieces of pyrex glass with silver ions and without silver ions, respectively, which were etched *in situ* on the carbon film in dilute HCl. The piece shown in Fig. 1d was wider and less uniform in thickness across its width; consequently, the central portion is dark.

The dark areas in Fig. 1, a and c, result from more scattering of electrons by the phase in which silver is concentrated, which is probably the borate phase. An ion exchange study (*4*) of pyrex glass showed that 95 percent of the sodium ions were in one phase, in agreement with the concentration of the silver in one phase shown in Fig. 1.

Fragments of the soda-lime glass were examined after silver exchange in the same way as the pyrex, but no structure was seen in this glass. Figure 1e is a photograph of the edge of a large splinter of the soda-lime glass with silver ions. Indirect evidence from ionic transport measurements (*8*) indicates that this particular glass does not separate into two phases, in agreement with the microscopic observations.

After the silver was exchanged into either glass, the glass was a light yellow color. However, the absorption spectrum of the glasses showed no trace of an absorption peak near the wavelength of 0.4 $\mu$m; this peak is characteristic of silver particles (*9*). Since the reduction of only a very small fraction of the silver ions to atoms and their agglomeration to particles would show an absorption band, essentially all of the silver is in ionic form. The yellow color results from an intense absorption band related to silver ions (*10*) at a shorter wavelength (about 0.24 $\mu$m).

Two mechanisms have been proposed for phase separation in glasses. In the first, small regions of the second phase nucleate and then grow by transport of material, as is observed in many conventional phase transformations. In the second, the homogeneous phase changes continuously and uniformly into two different phases whose compositions become progressively more dissimilar. The scale or "wavelength" of this "spinodal decomposition" is usually very small and leads to two interconnected and continuous structures. However, morphology does not always provide conclusive evidence for the mechanism of separation, since the continuous structure often breaks up into discrete particles in later stages of its growth, and there is some evidence for the conversion of particles to a continuous structure (*11, 12*). In spite of these uncertainties the separation shown in Fig. 1 probably resulted from a nucleation and growth mechanism, since it seems unlikely that aging of a continuous structure would lead to such small particles. The morphology observed here for pyrex is similar to that found in thin barium silicate films by Seward *et al.* (*12*); these authors also give an extensive discussion of the relation between mechanism of separation and morphology in phase separation of glasses.

The present technique of heightening the contrast between phases should be applicable to other materials in which a heavy ion can be exchanged for a lighter one. Segregation of ions at structural features in brittle materials could also be studied by preparing samples according to the method described in this report. Since this preparation does not involve mechanical or chemical thinning, it is more likely to preserve features of interest.

R. H. DOREMUS
A. M. TURKALO
*General Electric Research and Development Center, Schenectady, New York 12301*

**References**

1. M. E. Nordberg, *J. Amer. Ceram. Soc.* **27**, 299 (1944).
2. R. J. Charles, *ibid.* **47**, 559 (1964).
3. W. Vogel, *Struktur und Kristallisation der Gläser* (VEB Deutscher Verlag für Grundstoffindustrie, Leipzig, 1965).
4. R. H. Doremus, *J. Phys. Chem.* **72**, 2665 (1968).
5. H. M. Laska, R. H. Doremus, P. J. Jorgensen, *J. Chem. Phys.* **50**, 155 (1969).
6. W. Vogel, *Struktur und Kristallisation der Gläser* (VEB Deutscher Verlag für Grundstoffindustrie, Leipzig, 1965), p. 78.
7. A. M. Turkalo, *J. Amer. Ceram. Soc.* **51**, 470 (1968).
8. R. H. Doremus, *J. Electrochem. Soc.* **115**, 181 (1968).
9. ———, *J. Chem. Phys.* **42**, 414 (1965).
10. J. H. Schulman and W. D. Compton, *Color Center in Solids* (Macmillan, New York, 1962), p. 305.
11. W. Haller, *J. Chem. Phys.* **42**, 686 (1965).
12. T. P. Seward, D. R. Uhlmann, D. Turnbull, *J. Amer. Ceram. Soc.* **51**, 634 (1968). There are references to several other studies of phase separation in silicate glasses in this article.

22 January 1969

## Lunar Thermal Anomalies: Infrared Observations

Abstract. *The lunar craters Tycho, Copernicus, and Aristarchus have been observed during lunar night at wavelengths between 3 and 14 microns. After an initial fast decrease to a color temperature of 220°K, the temperature remains nearly constant through the lunar night. The data suggest that these thermal anomalies (craters) contain hot and cold regions with the hot portions constituting 2 to 10 percent of the area and probably thermally connected to a subsurface temperature of about 200°K.*

Infrared observations of the moon made mostly in the 8- to 14-$\mu$ atmospheric window have delineated the macroscopic thermal behavior of the lunar surface (*1*). These observations have shown that the surface temperature drops from about 390°K at noon to about 90°K before dawn. The form of the cooling curve is determined by the thermal inertia $(\kappa\rho C)^{1/2}$, and the observed 8- to 14-$\mu$ brightness temperatures indicate that this parameter has a value of 0.001 to 0.002. Observations of the cold limb at 20 $\mu$ (*2*) have confirmed the 90°K and support the very low thermal inertia (of .001 or less). Ordinary rocks such as granite and basalt have thermal inertias near 0.05. Low inertia of the lunar surface has been taken as evidence for an insulating dust layer covering the surface.

Additional information about thermal properties of the moon's surface was gained through the discovery by Shorthill of lunar thermal anomalies. The craters Aristarchus, Copernicus, and Tycho cool much less rapidly than their surroundings during eclipse (*3*). Shorthill and Saari (*4*) observed approximately 1000 such eclipse anomalies of which the great rayed craters are the outstanding examples.

Observations of thermal anomalies

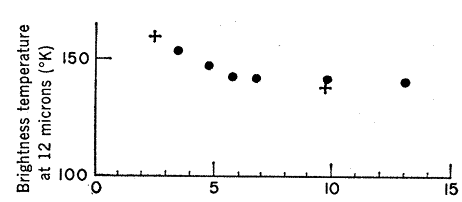


Fig. 1. Brightness temperature of Tycho at 12 $\mu$ as a function of time after sunset. (Circles) August 1968 lunation; (crosses) March 1969.

Table 1. Summary of the effective wavelengths, fluxes, and brightness temperatures for Tycho and Copernicus observed on March 14.7. The color temperature of Tycho is 230°C and that of Copernicus is 200°K.

| Effective wavelength ($\mu$) | Flux (watt/cm² ster $\mu$) | Brightness temperature (°K) |
|---|---|---|
| | *Tycho* | |
| 3.8 | $8.1 \pm 1.0 \times 10^{-8}$ | 199 |
| 4.9 | $1.2 \pm 0.2 \times 10^{-6}$ | 190 |
| 12 | $2.6 \pm 0.2 \times 10^{-5}$ | 160 |
| | *Copernicus* | |
| 4.9 | $3.0 \pm .05 \times 10^{-7}$ | 176 |
| 12 | $1.1 \pm 0.2 \times 10^{-5}$ | 143 |

made during lunar night at effective wavelengths of 3.8, 4.9, and 12 $\mu$ show that, although the brightness temperatures of the anomalies at long wavelengths do drop to low values at night, the color temperatures are much higher and are compatible with approximately 10 percent of the crater area radiating at the higher temperature.

The most spectacular thermal anomaly is the rayed crater Tycho. Figure 1 shows the 12-$\mu$ brightness temperature of Tycho observed during the August 1968 lunation. The midday temperature (5) of Tycho is 365°K and 3 days after sunset the 12-$\mu$ brightness temperature dropped to 160°K. During the remainder of the night the brightness temperature only falls to about 140°K.

The angular diameter of the beam used on these observations is 26 seconds of arc which corresponds to a distance of 48 km on the moon. The angular diameter of Tycho is about 50 seconds of arc; the anomaly therefore fills our beam. The reference photometer beam is thrown to a position 52 seconds of arc away. The signal to noise from Tycho at 12 $\mu$ and in a bandwidth of 3 $\mu$ is of the order of 500 in an integrating time of 1 second. Because of the large signal to noise it was possible to obtain a spectrum of Tycho by using a spectrometer with $\lambda/\Delta\lambda = 100$. The spectrum shows that, although the brightness temperature at 12 $\mu$ is 145°K, the color temperature is about 200°K (Fig. 2). These values may be reconciled if one assumes that approximately 10 percent of the surface area is at 200°K and that the remainder is at a much lower temperature (perhaps the 100°K midnight temperature). The relatively high color temperature suggested that the brighter anomalies might be observable at shorter wavelengths. Consequently we constructed a multifilter system in which the effective observing wavelengths could be changed from 3.8 to 4.9 or to 12 $\mu$ by mechanical means, without altering the position of the optical beam. It was therefore possible to locate a given anomaly on the dark moon by using the 12-$\mu$ wavelength and then to shift to short wavelength and integrate on the much weaker signal. Tycho and Copernicus were observed on March 14.7, 1969 and Tycho Copernicus, and Aristarchus on March 21.9 (see Fig. 3). The quantity $\eta$ is the effective emissivity for a crater that fills our beam. Both Tycho and Copernicus are larger than our beam but Aristarchus is smaller.

The absolute fluxes (Table 1) are determined by comparison with the star $\beta$ Pegasi. Table 2 summarizes the values of the color temperatures, emissivities, and cooling times. The fact that $\eta$ is between 0.02 and 0.1 indicates that only this fraction of the crater area is radiating at the color temperature.

The geometric scale of the structure of hot and cold regions cannot be determined from our observations. Maps of Tycho and Copernicus with a resolution of 12 seconds of arc made at 12 $\mu$, although revealing interesting structure, only show that the size of the individual hot regions is less than about 20 km. Ranger photographs have

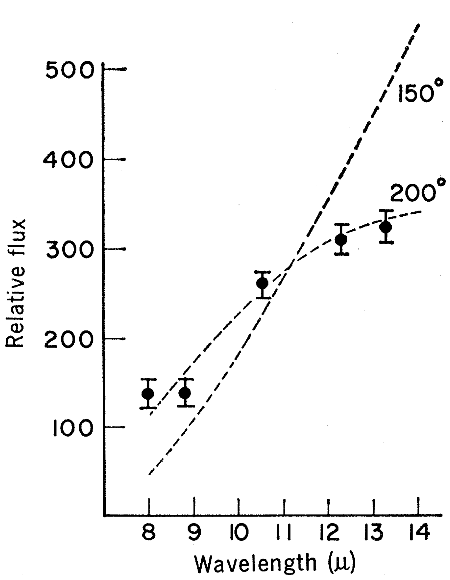


Fig. 2. The 8- to 14-$\mu$ spectrum of Tycho taken at new moon in August 1968. The points are fit by a blackbody curve with a color temperature of 200°K. For comparison, a blackbody curve with a color temperature of 150°K is shown.

Table 2. Color temperatures $T_C$ in degrees Kelvin, fraction of crater radiating $\eta$, and cooling time $\tau$ in days measured after sunset.

| Date | $T_C$ (°K) | $\eta$ | $\tau$ (days) |
|---|---|---|---|
| | *Tycho* | | |
| March 14.7 | 230 | 0.10 | 2.5 |
| March 21.9 | 220 | 0.035 | 9.7 |
| | *Copernicus* | | |
| March 14.7 | 200 | 0.08 | 1.7 |
| March 21.9 | 195 | 0.02 | 8.9 |
| | *Aristarchus* | | |
| March 21.9 | 200 | 0.03* | 6.9 |

* Not corrected for crater failing to fill beam.

shown the presence of rocks of various sizes in and near the rayed craters. It is tempting to postulate that these boulders are the hot regions and are displaying thermal properties very much like terrestrial materials. If this is the explanation, one must conclude that there has not been time to cover the rocks with an insulating layer since Tycho and Copernicus were formed. In this connection, it is worth noting that although Kepler is an outstanding rayed crater, it is an inconspicuous thermal anomaly, which suggests that this crater may either be older or have a smaller fraction of bare rock.

If the rocks have values of $(\kappa\rho C)^{1/2}$ as large as 0.05 (like basalt), then

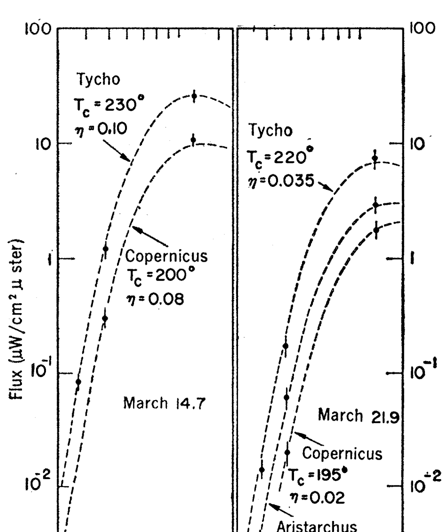


Fig. 3. Absolute fluxes as a function of wavelength from Tycho, Copernicus, and Aristarchus. Curves are blackbody spectra giving a good fit to the color temperature; $T_C$, color temperature; $\eta$ fraction of the crater radiating. Results are summarized in Table 2.

during the lunar night the thermal wave can penetrate about 1 m. One would therefore expect that rocks 1 m or larger in size would be effectively clamped after several days to the temperature of the subsurface of the moon. This temperature is believed to be about 220°K, which is close to our observed color temperatures of 200° to 230°K. The decrease of $\eta$ with increasing cooling time may arise because the smaller rocks cool first.

D. A. ALLEN

*The Observatories, Cambridge University, Cambridge, England*

E. P. NEY

*School of Physics and Astronomy, University of Minnesota, Minneapolis 55455*

**References and Notes**

1. W. M. Sinton, in *Physics and Astronomy of the Moon*, Z. Kopal, Ed. (Academic Press, New York, 1962), pp. 407–428.
2. F. J. Low, *Astrophys. J.* **142**, 806 (1965).
3. R. W. Shorthill, H. C. Borough, J. M. Conley, paper presented at the 17 June 1960 meeting of the Astronomical Society of the Pacific.
4. R. W. Shorthill and J. M. Saari, *Science* **150**, 210 (1965); J. M. Saari and R. W. Shorthill, *Sky and Telescope* **31**, 327 (1966); ———, T. K. Deaton, Boeing Document D1-82-0533, July 1966; ———, *Icarus* **5**, 635 (1966).
5. J. M. Saari and R. W. Shorthill, *Isothermal and Isophotic Atlas of the Moon, NASA CR-855*, (NASA, Washington, D.C., 1967).
6. We thank N. Woolf and G. Burnett for discussions, R. Maas and J. Stoddart for development of the infrared systems, and R. Maas and A. Ney for assistance in making the observations. Supported by NASA grant NGL-24-055-008. One of us (D.A.A.) acknowledges financial support from the Science Research Council and Cambridge University. Observations were made with the 30-inch telescope at O'Brien Observatory, University of Minnesota.

1 April 1969

## Olmec Cave Paintings: Discovery from Guerrero, Mexico

Abstract. *A cave in Guerrero, Mexico, investigated in 1968, contained previously unreported Olmec paintings. These paintings, some of the oldest known in Mesoamerica, are stylistically similar to Olmec art from the site of LaVenta, on Mexico's Gulf Coast, but contain several important glyphic motifs never previously known to have existed at this time level. The iconography of the paintings confirms several important hypotheses concerning basic concepts of Olmec religion; the cave itself was probably a shrine to water and fertility. Several pre-Hispanic textile fragments found in the cave are probably from a later culture period.*

A series of paintings in Juxtlahuaca cave, Guerrero, Mexico (Fig. 1), reinvestigated in 1966, were identified as belonging to the art style of the Olmec culture (*1*), Mesoamerica's first civilization and first great art style. These sophisticated paintings, acclaimed as the "oldest paintings of the New World," are located on walls deep within the cave and include representations of several human figures, a jaguar, and a serpent. Until the discovery of the Juxtlahuaca paintings, Olmec art was known in primarily three forms: (i) large monumental stelae and colossal stone heads, (ii) small portable carvings in jade, jadeite, or serpentine, and (iii) in various ceramic forms.

Today, archeological pieces in the Olmec style are known from widely dispersed areas of Mexico, Guatemala, and even Central America, and the identification of the Juxtlahuaca paintings as Olmec has opened an entirely new facet in the study of Olmec culture. The actual heartland of this culture seems to be Mexico's Gulf Coast, in particular the states of Veracruz and Tabasco. Recent archeological work at two major Olmec sites in this region, San Lorenzo and La Venta (Fig. 1), has yielded a new series of radiocarbon dates which places the Olmec culture between 1200 and 600 B.C. (*2, 3*), earlier than ever suspected (*4*). With the exception of the site of Chalcatzingo (Fig. 1) (*5*) in Mexico's central highlands and a newly discovered stelae near Arcelia, Guerrero, monumental Olmec stone carvings are restricted to the Gulf Coast sites. Olmec sites in the central highlands also appear to lack the ceremonial architecture of Gulf Coast sites, but have yielded a greater abundance of smaller archeological objects such as ceramics and jade carvings (*6, 7*).

In November 1968, as a continuation of my studies of Olmec culture, a cave near Chilapa, Guerrero, was investigated (*8*); it contained a number of wall paintings of various types, most of which are unquestionably Olmec. The area in which the cave is located is only about 20 miles (12.5 km) north of Juxtlahuaca cave; because the indigenous villages of this area still retain the Nahuatl language, the cave is known locally as Oxtotitlan (Fig. 1). The cave sits high on a hillside, overlooking the valley of the Río Atentli. Unlike Juxtlahuaca cave, the Oxtotitlan paintings occur in the mouth of the cave, in two large grottoes which open widely onto a broad cliff face. The largest of the paintings occurs on the cliff face in front of the grottoes. Whereas one of these is faded and virtually indistinguishable, the second is well preserved. This painting (Fig. 2) occurs high on the cliff, above the mouth of the south grotto (*9*); it represents a human figure seated upon a large jaguar-monster head. The figure wears an owl headdress mask, a feathered cloak, a jade pectoral, jade ornaments on his arms, legs, and feet, and a fringed skirt. The jaguar-monster head is reminiscent of the large stone jaguar-monster altars found at Olmec sites on the Gulf Coast. These stone altars are usually carved with a deep niche at their base which represents the jaguar-monster's mouth and iconographically probably also a cave. The jaguar-monster mouth-cave association has been noted at Chalcatzingo (*5*, relief ix, pp. 489–90) in connection with actual caves; and it is interesting, therefore, to note that the Oxtotitlan painting of the jaguar monster occurs above the mouth of the south grotto, which suggests a similar association. The main colors of this painting are red, ocher, and blue and it is approximately 5 by 7 feet (1.5 by 2.1 m) in size.

Within the north grotto of Oxtotitlan are a series of Olmec paintings executed primarily in black. Among these paintings are several profile faces with the baby-face mouth, a characteristic of Olmec art. Associated with one of these faces is a glyphic motif common in later Mesoamerican art, the speech scroll; it antedates any other examples by nearly 1000 years, and is the only


Fig. 1. Olmec sites.